Ceramics International **24** (1998) 527–532

PII: S0272-8842(98)00052-7
0272-8842/98 $19.00 + .00

Colloidal Processing of Calcium Carbonate

G. Tarì & J. M. F. Ferreira

Department of Ceramics and Glass Engineering, University of Aveiro, 3810 Aveiro, Portugal

(Received 17 March 1997; accepted 29 May 1997)

Abstract: Two natural calcium carbonate ($CaCO_3$) powders were dispersed in aqueous media and their colloidal processing ability was studied. In absence of dispersant, electrophoretic measurement showed a very low surface charge density on calcium carbonate particles that do not allow the preparation of stable suspensions suitable for the casting process. However, the addition of an appropriate dispersant caused a significant increase of the surface charge density of $CaCO_3$ powders, enabling the preparation of relatively dense suspensions. Calcium carbonate suspensions with very high solid loading (60 vol%) and viscosities low enough for casting operations could be prepared. Rheological measurements and casting experiments were performed in order to correlate the flow characteristics of the slips with the particle ability towards packing. Very high green and sintered densities were obtained, reaching more than 74 and 95% of the theoretical density, respectively. Considering the availability, low price and the processing ability of calcium carbonate by colloidal techniques, as revealed in this work, this material can represent a useful option for ceramic manufacture. © 1998 Elsevier Science Limited and Techna S.r.l.

1 INTRODUCTION

Calcium carbonate ($CaCO_3$) is a material widely used for many applications in different industrial fields such as Portland cement,[1] soda-lime glassware, smelting of iron ore in foundry. In a near colloidal size, calcium carbonate is widely employed as a filler in paper and plastics industries.[2,3]

In the domain of ceramic science, calcium carbonate has been considered as a flux in earthenware and pottery production.[4] Recent applications as a bioceramic material for implantation purposes have been proposed, due to its biocompatibility and bioresorbability properties.[5,6] Although this ceramic material does not closely match the composition of the mineral bone as hydroxyapatite does, it has some interesting advantages compared to hydroxyapatite. Namely, it is a simple and inexpensive raw material, and sintered bodies of $CaCO_3$ are mechanically stronger. The typical decomposition reaction with the formation of CaO and CO_2 starting at a relatively low temperature (700°C under air) can be avoided during sintering by using a CO_2 atmosphere or sintering aids like Li_3PO_4.[7] Besides its potential use as bioceramic material, calcium carbonate can represent a useful option when a cheaper material with complex shapes is required, provided that the mechanical performance and/or temperature and chemical environment conditions are not extreme.

The aim of this work was to study the processing ability of the calcium carbonate by colloidal techniques, namely slip casting, and obtain knowledge for further processing of ceramic components based on this material.

2 EXPERIMENTAL PROCEDURE

2.1 Materials and slip preparation

Two commercial calcium carbonate powders (M1 and Mα, Mineraria Sacilese, Italy) were used. XRD analysis (XDMAX, Rigaku Inc., USA) revealed that calcite was the only crystalline phase present in both powders. The chemical composition of the calcium carbonate used in this study, as furnished by the supplier, and the pH of the

Table 1. Sample's description, pH of the suspensions and chemical analysis of the calcium carbonates used (as furnished by the supplier)

	40 vol%		50 vol%		55 vol%		60 vol%	
pH	M1	Mα	M1	Mα	M1	Mα	M1	Mα
	9.1	9.1	9.2	9.1	9.1	9.1	9.0	8.9
M1/Mα	$CaCO_3$ 99.6%	SiO_2 0.02%	Fe_2O_3 0.005%	Al_2O_3 0.005%	$MgCO_3$ 0.33%	S ‹60 ppm	Mn ‹10 ppm	Cr ‹5 ppm

suspensions in their full stabilised state are shown in Table 1. Despite their natural origin, these products were relatively high purity containing more than 99% of $CaCO_3$. The SEM micrographies (Hitachi S-4100, Japan) of the calcium carbonate M1 and Mα are presented in Fig. 1(a) and (b), respectively. Both powders exhibit similar morphological characteristics, consisting of polyfaced particles with rounded corners. Initiated cleavage cracks characteristic of the calcite materials can be also observed in some particles at high magnification. These characteristics are not surprising since the powders M1 and Mα, are different size fractions of the same raw material prepared by grinding. This can be confirmed by the particle size distributions of the powders (Mastersizer 4, Malvern Intr., UK) reported in Fig. 2.

The dispersant used was an ammonium polycarbonate (Targon 1128, BK Ladenburg, Germany) that in previous work[8] was revealed to be very efficient in stabilising calcium carbonate suspensions. The solid loading was varied from 40 up to 60 vol%. For each powder and solid loading tested, the amount of dispersant that gave the lowest viscosity was determined.

Experimentally, the suspensions were prepared by first mixing water and dispersant for 1 min with a mechanical stirrer. Then the powder was progressively added and kept under stirring for a further 20 min. Deagglomeration of the calcium carbonate was performed by ball milling in a plastic container for 16 h, using silicon nitride balls as grinding media (diameter = 15 mm). Finally, the balls were removed and the suspensions homogenised for 5 h by rolling in the same plastic container.

2.2 Slip characterisation

Electrophoretic analysis was carried out with a Zetasizer 4 (Malvern Instr., UK). The zeta potential was detected from the motion of particles caused by an external electric field. Measuring the rate of the motion (electrophoretic mobility) of the particles and using the Smoluchowski equation, the zeta potential of the particles was determined.[9]

The suspensions were characterised electrophoretically after dilution of the concentrated $CaCO_3$ slurries in an aqueous electrolyte solution (KCl in de-ionized water, 0.001 M) up to solid concentrations less than 0.01 wt%. The pH was measured with a pH meter (Corning 240, UK), calibrated with buffer solutions (pH 7, 10 Merck, Germany) and pH adjustment was done with aqueous solution of HCl or NaOH (0.1 and 0.01 M).

Rheological measurements were carried out with a rotational controlled stress rheometer (Carri-med 500 CSL, UK), immediately after the 5 h slip con-

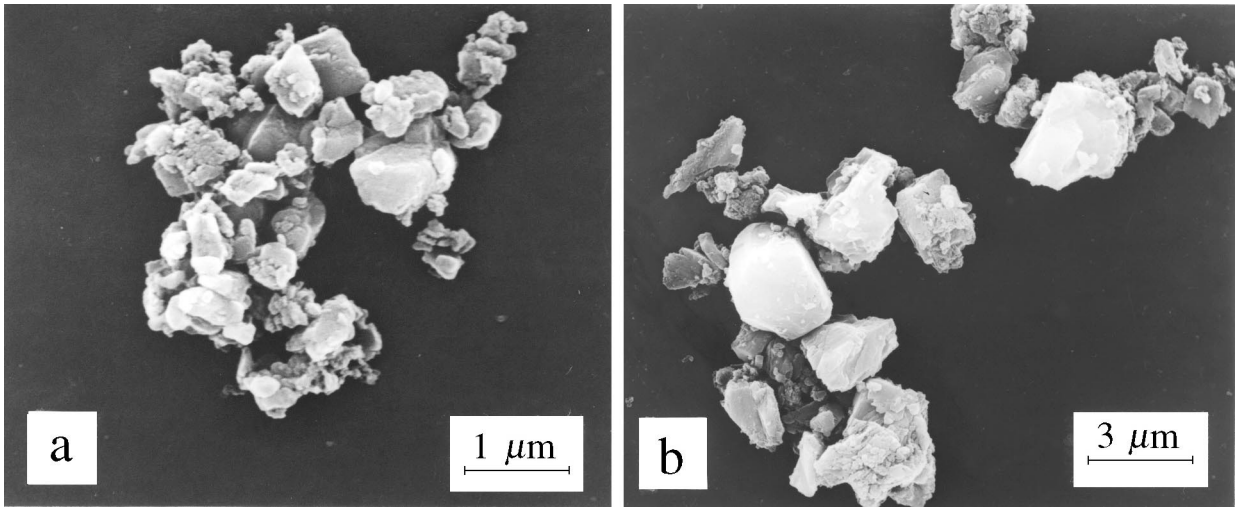

Fig. 1. SEM micrographs of the starting calcium carbonate powders: (a) M1 and (b) Mα.

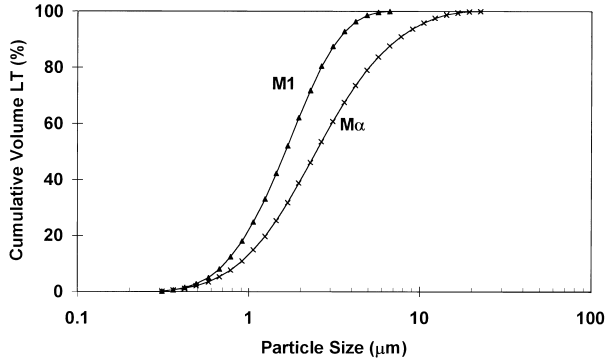

Fig. 2. Particle size distribution of the starting calcium carbonates powders.

ditioning at strictly controlled temperature of 20°C. The measuring configuration adopted was a concentric coaxial cylinder and multi-step shear measurements (10 points, max. equilibrium time of 3 min) were performed in the shear rates range from about 0.1 s^{-1} until 550 s^{-1}. Before starting a measurement, pre-shearing was performed at high shear rate for 1 min followed by at rest of 2 min in order to transmit the same rheological history to all the suspensions tested.

2.3 Green and sintered body characterisation

From each suspension, three cylindrical samples (diameter = 28 mm, thickness≅4 mm) were formed by pouring the slip into plastic rings based on an adsorbent plaster plate. The slip cast samples so-obtained were dried in an oven at 120°C for 24 h, and then sintered at 850°C in a vertical tubular furnace under 1 atmosphere of CO_2 (flow rate = 3-litre min^{-1}). The firing schedule adopted was 5°C min^{-1} from 20°C up to 820°C, 1°C min^{-1} up to the sintering temperature, followed by a holding time of 2 h, and free cooling down.

Densities of the green and sintered bodies were measured by the immersion method in mercury.

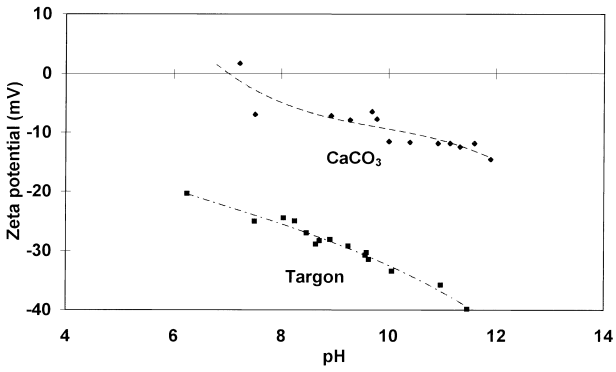

Fig. 3. Zeta potential curves of calcium carbonate powders without and with addition of dispersant (Targon 1128).

3 RESULTS AND DISCUSSION

3.1 Slip characterisation

Figure 3 shows the zeta potential curves of the $CaCO_3$ powders in the presence and in the absence of the surface active agent. It can be seen that the surface charge density of calcium carbonate particles is very low ($\zeta \approx 10$ mV). Without dispersant added, the isoelectric point (IEP) appears to be located at pH 7.3. However, this result should be regarded with caution since the solubility of calcium carbonate strongly increases with decreasing pH. For pH values lower than pH ≈ 7 it was not possible to measure the electrophoretic mobility owing to rapid dissolution.[10] In these conditions, the ionic strength increases and consequently the zeta potential should decrease even if the surface charge was unchanged. The low negative surface charge density might be due mainly to the relative concentrations of calcium and carbonate ions in solution, since they are the potential determining ions.[11] Both the magnitudes of the zeta potential and the IEP of the calcium carbonate particles are in close agreement with the findings of other authors.[11,12]

When Targon was added the repulsive forces among particles increase considerably, as can be depicted from Fig. 3. The negative zeta potential increases and the presence of Targon also enabled electrophoretic measurements further in the acidic direction, suggesting that the solubility of the $CaCO_3$ particles might have been diminished by the adsorbed polyelectrolyte chains. The composition of the functional groups of this dispersant might have some relation with its efficiency. However, colloidal instability and almost complete dissolution of the dispersed $CaCO_3$ powder occurred before any IEP could be detected. Zeta potential measurements were difficult in the low pH region when the intensity detected by the photomultiplier decreased to about 25% of the maximum counting rate observed at higher pH values.

Figure 4(a) and (b) show the viscosity curves of the calcium carbonate suspensions at different solid loading and prepared with M1 and Mα powders, respectively. At low shear rates, all the slips show a typical shear thinning behaviour with a decreasing viscosity with increasing shear rate. In the case of suspensions prepared with M1, this pseudo-plastic behaviour is observed over all shear rate range tested, whereas in the case of Mα, they become progressively shear thickening as the shear rate increases. Further, it can be observed that the viscosity level of the suspensions prepared with

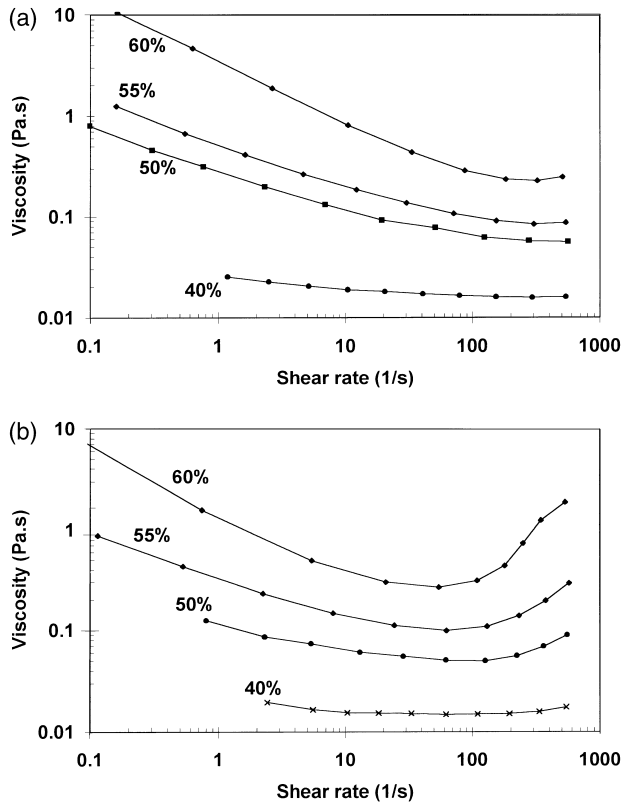

Fig. 4. Viscosity curves of the $CaCO_3$ suspensions at different solid loading: (a) M1 and (b) Mα.

M1, the finer powder tested, is generally higher than in the case of Mα. Overall, these flow characteristics become more evident as the solid loading increases.

The shear thinning behaviour is usually associated with the slurry structure. At low shear rates, liquid is immobilised in void spaces within flocs and the floc network. As the shear rate is increased, the flocs and floc network break down and the entrapped liquid is released and a more ordered structure in the flow direction is formed.[13] The higher viscosity and the more pronounced shear thinning character of calcium carbonate M1 can be attributed to its higher specific surface area. The effective volume of one particle is given by the sum of the bulk particle and the thickness of the adsorbed or solvated layer. For a given solid loading, the number of the suspended particles is considerably higher for M1. Hence, for the same solid loading, the effective volume fraction should be higher in the case of calcium carbonate M1 and, consequently, an increase of the viscosity level is expected and observed, in comparison with Mα. At low shear rate the interparticle forces still dominate the particulate system. However, the agitation action can gradually break down this structure by overcoming the attractive energy corresponding to the secondary minimum and thus the viscosity of the suspension decreases. At high shear rates, the hydrodynamic interactions between particles become dominant and the number of collisions per unit time increases. On the other hand, for particles to slide over each other they have to increase their average separation distance, especially when coarse particles are present. This causes an apparent increase in solid volume fraction that is responsible for the increased viscosity, i.e. shear thickening,[14] which tends to be more pronounced in the case of Mα.

3.2 Green and sintered body characterisation

Table 2 summarises the slip cast and sintered density of samples at different solid loading. It can be seen that for both powders tested, the density of the green compacts steadily increases with increasing solid loading, reaching a maximum value of 73.8% of the theoretical density, in the case of M1 at 60 vol%. However, for the other solid loading tested, the density of the slip cast bodies tends to be slightly higher with Mα powder than with M1. These results can be explained in terms of solid loading and particle size distribution effects on packing density of slip cast bodies.

An increasing number of particles in suspension leads to higher viscosities, diminution of the segregation phenomena, and to a closer mutual approach between particles in suspension and so, to a higher cast density in the wet state. In analogy with alumina and silicon carbide powders,[15,16] these results suggest that two solid loading regimes (low and high) control the packing behaviour during the forming process. At low solid loading, the high amount of water available and the lower frequency of collisions between particles enables the formation of relatively thick hydrated layers

Table 2. Relative density of the green and sintered bodies at different solid loading (the theoretical density of $CaCO_3$ was assumed to be 2.71 g cm^{-3})

Solid loading (vol%)	M1				Mα			
	40	50	55	60	40	50	55	60
ρ(g cm^{-3})	1.79	1.85	1.90	2.00	1.84	1.87	1.95	1.99
TD (%)	66.1	68.3	70.1	73.8	67.9	69.0	72.0	73.4
ρ(g cm^{-3})	2.57	2.56	2.57	2.58	2.42	2.43	2.46	2.46
TD (%)	94.8	94.5	94.8	95.2	89.4	89.7	90.8	90.8

surrounding the particles. This higher interaction size persists during the deposition stage, and even in the wet cake, resulting in lower packing densities. In addition, the segregation phenomena are enhanced at low solid concentration and further decreases the ability of particles towards packing. At high solid loading, the thickness of the hydrated layer around particles is reduced due to the lower amount of water available and to the higher frequency of collisions between particles during slip preparation. On the other hand, the segregation phenomena become less and less important as the solid loading increases. Assuming that no air is entrapped within the green compact, a higher packing density is expected in comparison with the situation at low solid loading.

The small difference in packing behaviour between M1 and Mα might be related to the shape of their particle size distributions (PSDs). In fact, Fig. 2 shows that powder M1 has a narrower PSD than Mα. Many studies[17–19] have demonstrated that broader and/or bimodal PSDs are favourable in terms of the packing performance, since fine particles can occupy the interstitial pore spaces between the coarser ones. This higher packing ability of the Mα powder should also occur in suspension as can be depicted from the previous rheological characterisation. Besides its lower specific surface area, the lower viscosity and the shear-thickening behaviour of Mα suspensions give further evidence about the ability of this powder to packing.

Results of sintered body density are also reported in Table 2. It can be observed that the density is always higher in the case of M1, despite the slightly lower density in green state. This results can be explained as follows. The finer M1 particles are more reactive than the coarser Mα, owing to the higher specific surface area. So, the high reactivity of M1 particles enhances solid state reactions with an increased densification level during sintering.[20] For each powder, an increasing trend of the sintered density with solid loading is also observed, like in the green state, suggesting that the particle packing influences the densification during sintering.

4 SUMMARY AND CONCLUSION

- The naturally low surface charge density of calcium carbonate in aqueous media can be enhanced by using an anionic dispersant based upon ammonium polycarbonates (Targon 1128).
- Colloidal processing of calcium carbonate revealed to be very easy. It was possible to prepare suspensions with very high solid loading (60 vol%) and viscosities low enough for casting operations. High dense slip cast bodies were obtained, reaching about 74% of the theoretical density, which after sintering attain densification levels of about 95%.
- Considering the availability, low price and the processing ability of calcium carbonate by colloidal techniques, this material represents a useful option for ceramic manufacture.

ACKNOWLEDGEMENT

This work was supported by JNICT contract no. PBIC/C/CTM/1968/95.

REFERENCES

1. BURLAMACCHI, L., *Capire il Calcestruzzo*. Hoepli S.p.A., Milano, 1994, Chap. 2, p. 13.
2. ROBERTS, J. C., *Paper Chemistry*, 2nd edn. Chapman & Hall, Glasgow, 1996, p. 196.
3. ALPER, J. & NELSON, G. L., *Polymeric Materials—Chemistry for the Future*. American Chemical Society, Washington, 1989, p. 39.
4. RYAN, W. & RADFORD, C., *Whiteware Production, Testing and Quality Control*. Pergamon Press, Oxford, 1987, p. 13.
5. OHGUSHI, H., OKAMURA, M., YOSHIKAWA, T. & INOUE, K., Bone formation process in the porous calcium carbonate and hydroxyapatite. *J. Bio. Mater. Res.*, **26** (1992) 885–895.
6. DRIESSENS, F. C. M., Chemistry of Calcium Phosphate Cements. *Proc. of 4th Euro-Ceramics, Vol. 8—Bioceramics*, ed. A. Ravaglioli. Gruppo Editoriale Faenza Editrice S.p.A., Riccione, Italy, 1995, 77–83.
7. TÉTARD, F. & BERNACHE-ASSOLLANT, D., Calcium Carbonate Densification with Li_3PO_4. *Proc. of 4th Euro-Ceramics, Vol. 8—Bioceramics*, ed. A. Ravaglioli. Gruppo Editoriale Faenza Editrice S.p.A., Riccione, Italy, 1995, 169–176.
8. FERREIRA, J. M. F., TARI, G. & TOUCHAL, S., Dispersion, stabilisation and casting of calcium carbonate suspension. In *Proc. 5th E. Cer. S.*, Versailles, France, 1997, pp. 289–292.
9. HUNTER, R. J., *Foundations of Colloid Science*, Vol. 1, Chap. 9. Oxford University Press, New York, 1987, p. 557.
10. PERRY, R. H., GREEN, D. W. & MALONEY, J. O., *Perry's—Chemical Engineers' Handbook*, 6th edn. McGraw-Hill, Singapore, 1984.
11. CICERONE, D. S., REGAZZONI, A. E. & BLESA, M. A., Electrokinetic properties of the calcite/water interface in the presence of magnesium and organic matter. *J. Colloid Interf. Sci.*, **154** (1992) 423–433.
12. ALLAIN, C., CLOITRE, M. & PARISSE, F., Settling by cluster deposition in aggregating colloidal suspensions. *J. Colloid Interf. Sci.*, **178** (1996) 411–416.
13. SACKS, M. D., Properties of silica suspensions and cast bodies. *Am. Ceram. Soc. Bull.*, **63** (1984) 1510–1515.
14. PUGH, R. J. & BERGSTROM, L., *Surface and Colloid Chemistry in Advanced Ceramic Processing*. Surfactant science series Vol. 51. Marcel Dekker, New York, 1994, p. 216.

15. TARI, G., FERREIRA, J. M. F. & LYCKFELDT, O., Influence of stabilisation mechanism and solid loading on slip casting of alumina. *J. Eur. Ceram. Soc.*, **18** (1998) 479–486.
16. FERREIRA, J. M. F., A Interface SiC–Solução Aquosa e o Enchimento por Barbotina, Ph.D Thesis, University of Aveiro, Portugal, 1992.
17. FERREIRA, J. M. F. & DIZ, H. M. M., Effect of the amount of deflocculant and powder size distribution on the green properties of silicon carbide bodies obtained by slip casting. *J. Hard Materials*, **3** (1992) 17–27.
18. GERMAN, R. M., *Particle Packing Characteristics*. MPIF, Princeton, 1989, Chap. 8, p. 197.
19. TARI, G., FERREIRA, J. M. F., FONSECA, A. T. & LYCKFELDT, O., Influence of particle size distribution on colloidal processing of alumina. *J. Eur. Ceram. Soc.*, **18** (1998) 249–253.
20. REED, J. S., *Principles of Ceramic Processing*, 2nd edn. John Wiley & Sons, New York, 1994, p. 449.